Satellite and terrestrial spherical harmonic coefficients of the external gravitational potential do not match

Blažej Bucha[1]   Fernando Sansò[2]

[1]Department of Theoretical Geodesy and Geoinformatics
Slovak University of Technology in Bratislava
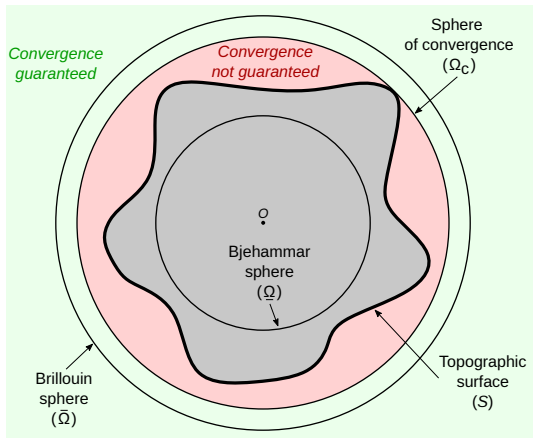blazej.bucha@stuba.sk

[2]Department of Civil and Environmental Engineering
Politecnico di Milano
fernandosanso060545@gmail.com

EGU General Assembly 2023, Vienna

Motivation

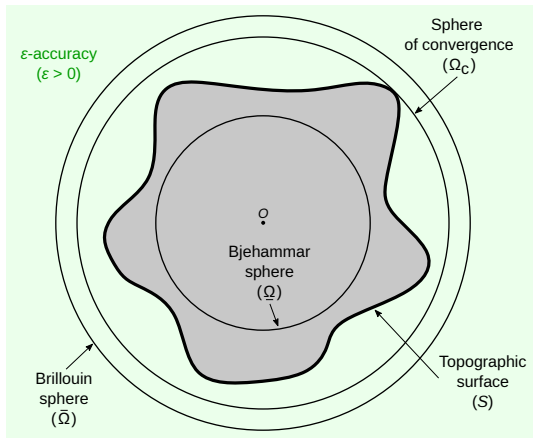$$V(r, \sigma) = \frac{GM}{\overline{R}} \sum_{n=0}^{N_S} \left(\frac{\overline{R}}{r} \right)^{n+1} \sum_{m=-n}^{n} \bar{V}_{nm}^S \, \bar{Y}_{nm}(\sigma) \tag{1}$$

- Uniform convergence for $N_S \to \infty$
- Likely divergence for $N_S \to \infty$ and realistic bodies
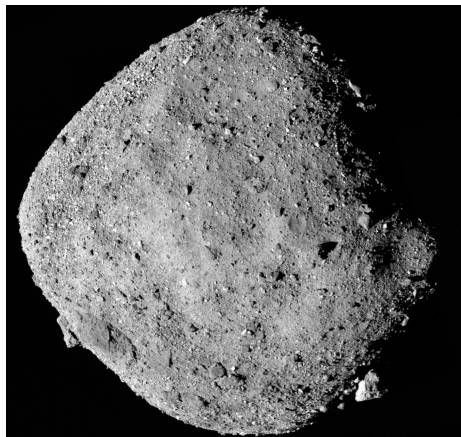- From gravity data above Ω_c (GRACE, GOCE, GRAIL, etc.)

$$V_{N_{\mathrm{T}}}(r, \sigma) = \frac{GM}{\underline{R}} \sum_{n=0}^{N_{\mathrm{T}}} \left(\frac{R}{r} \right)^{n+1} \sum_{m=-n}^{n} \bar{V}_{nm}^{\mathrm{T}}(N_{\mathrm{T}}) \, \bar{Y}_{nm}(\sigma) \qquad (2)$$

- Arbitrary ε-accuracy, $\varepsilon > 0$ (Runge–Krarup theorem)
- $\|V_{\mathrm{True}} - V_{N_{\mathrm{T}}}\|_{L_2(\omega)} = $ min on S
- $\bar{V}_{nm}^{\mathrm{T}}(N_{\mathrm{T}})$ depend on N_{T}
- From gravity data on S (terrestrial and altimetric gravity, etc.)

Model of Bennu

Bennu: Quick facts from Wikipedia

*Bennu as seen by NASA's OSIRIS-REx*
(https://www.nasa.gov)

- 1999: Discovered
- 2016: Launch of OSIRIS-REx
- 2020: Landing of OSIRIS-REx
- 2023 (September): Scheduled return of samples to Earth
- Mean diameter: 490 m
- 1:1800 cumulative chance of impacting the Earth in years between 2178 and 2290
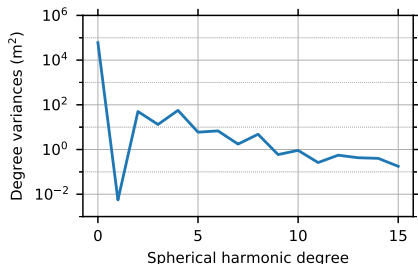
Bennu: Model

- **Shape**: Surface spherical harmonic expansion

$$r_{\mathrm{S}}(\sigma) = \sum_{n=0}^{15} \sum_{m=-n}^{n} \bar{r}_{nm}^{\mathrm{S}} \, \bar{Y}_{nm}(\sigma) \tag{3}$$

- **Density**: $1260 \ \mathrm{kg \ m^{-3}}$ (constant)
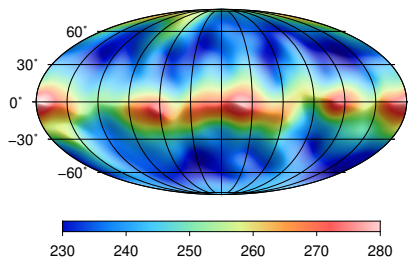
Degree-15 surface spherical harmonic expansion (m) derived from the polyhedral model due to [Nolan et al., 2013]
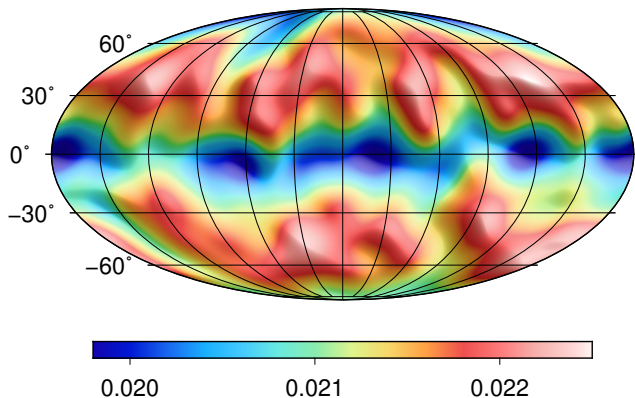

Spectrum of r_{S}

Reference potential

Reference potential

- Gravity forward modelling after [Fukushima, 2017]
- Spatial domain (independent of spherical harmonics)
- Reference values on Bennu's surface and on a Brillouin sphere
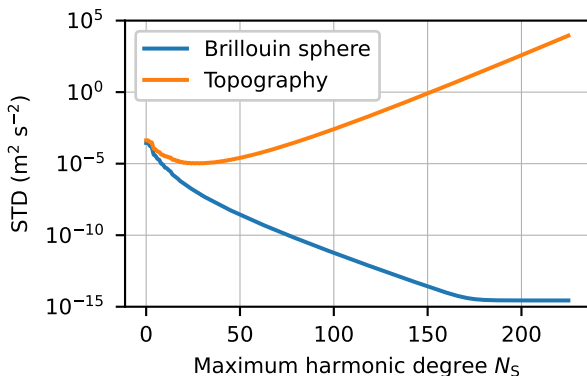

Reference gravitational potential on Bennu's surface ($\mathrm{m^2\,s^{-2}}$)
at the Gauss–Legendre grid corresponding to degree 255 (226×452 points).

Satellite series

Satellite series: Computation

- Spectral gravity forward modelling: $\bar{r}_{nm}^{\mathrm{S}} + \rho$ to $\bar{V}_{nm}^{\mathrm{S}}$
- Satellite coefficients $\bar{V}_{nm}^{\mathrm{S}}$ with any accuracy
- Shape r_{S} is limited to degree 15, but the potential series is infinite

Spatial-domain errors of the satellite series
as a function of maximum harmonic degree N_{S}.

Terrestrial series

Terrestrial series: Computation

To estimate the terrestrial series

$$V_{N_{\mathrm{T}}}(r, \sigma) = \frac{GM}{\underline{R}} \sum_{n=0}^{N_{\mathrm{T}}} \left(\frac{R}{r} \right)^{n+1} \sum_{m=-n}^{n} \bar{V}_{nm}^{\mathrm{T}}(N_{\mathrm{T}}) \, \bar{Y}_{nm}(\sigma), \tag{4}$$

we seek for the least-squares solution of the linear system

$$\frac{GM}{\underline{R}} \sum_{n=0}^{N_{\mathrm{T}}} \sum_{m=-n}^{n} \bar{V}_{nm}^{\mathrm{T}}(N_{\mathrm{T}}) \, \left(\bar{S}_{nm}(r_{\mathrm{S}}, \sigma), \bar{S}_{jk}(r_{\mathrm{S}}, \sigma) \right)_{L_2(\omega)}$$
$$= \left(V(r_{\mathrm{S}}, \sigma), \bar{S}_{jk}(r_{\mathrm{S}}, \sigma) \right)_{L_2(\omega)}, \quad (r_{\mathrm{S}}, \sigma) \in S, \tag{5}$$

where

$$\bar{S}_{nm}(r_{\mathrm{S}}, \sigma) = \left(\frac{R}{r_{\mathrm{S}}} \right)^{n+1} \bar{Y}_{nm}(\sigma), \tag{6}$$

$$(f, g)_{L_2(\omega)} = \frac{1}{4\pi} \iint\limits_{\omega} f(\sigma) \, g(\sigma) \, \mathrm{d}\omega(\sigma) \tag{7}$$

and ω is the unit sphere. Note that r_{S} depends on $\sigma = (\varphi, \lambda)$.

- Terrestrial series estimated for $N_{\mathrm{T}} = 0, 5, 10, \cdots, 65$
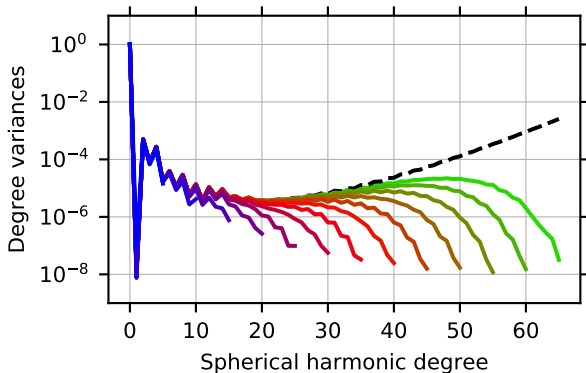
Spectra of the terrestrial solutions estimated for $N_{\mathrm{T}} = 5$ (the blue line), 10, ..., 65 (the green line) and of the satellite solution (dashed black line) on the Bjerhammar sphere.

It can be shown that

$$\lim_{N_{\mathrm{T}}\to\infty} \bar{V}_{nm}^{\mathrm{T}}(N_{\mathrm{T}}) = \left(\frac{\overline{R}}{\underline{R}} \right)^n \bar{V}_{nm}^{\mathrm{S}}. \tag{8}$$

That is, for $N_{\mathrm{T}} \to \infty$, the terrestrial series approaches the (possibly divergent!) satellite series but, at the same time, it can guarantee an arbitrary ε-accuracy, $\varepsilon > 0$!
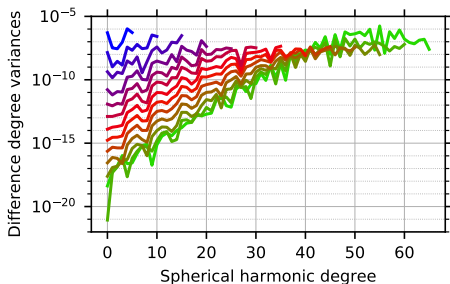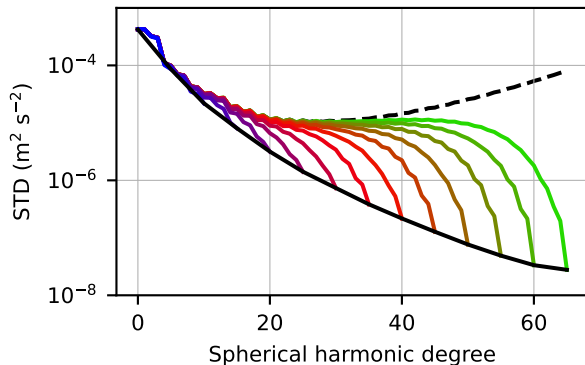

Difference degree variances between the terrestrial and satellite coefficients on the Bjerhammar sphere. The same colours are used as in the previous figure.
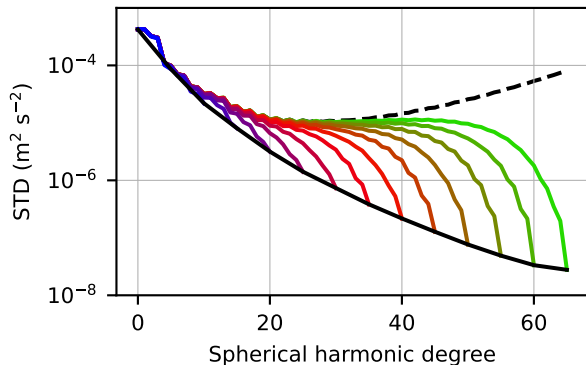
Spatial-domain errors of the terrestrial solutions (colour lines) and of the satellite solution (dashed black line) as a function of spherical harmonic degree on Bennu's surface.

Spatial-domain errors of the terrestrial solutions (colour lines) and of the satellite solution (dashed black line) as a function of spherical harmonic degree on Bennu's surface.

Evaluating partial sums from terrestrial models
below the sphere of convergence can be dangerous.

Conclusions

Conclusions

- In theory, we should distinguish between satellite and terrestrial potential series

- On the theoretical level, terrestrial series should be used exclusively up to their maximum degrees. Evaluation of partial sums near topography may be dangerous.

- With terrestrial series, we may loose the ability of the spectral decomposition, making spherical harmonics behave more like the spatial methods do

Notconclusions
(tempting but false conclusions)

- Since for any $P(r, \sigma)$ above S we have in $L_2(\omega)$ sense

$$
\begin{aligned}
V(P) &= \lim_{N_{\mathrm{T}} \to \infty} V_{N_{\mathrm{T}}}(P) \\
&= \lim_{N_{\mathrm{T}} \to \infty} \frac{GM}{\underline{R}} \sum_{n=0}^{N_{\mathrm{T}}} \left(\frac{R}{r} \right)^{n+1} \sum_{m=-n}^{n} \bar{V}_{nm}^{\mathrm{T}}(N_{\mathrm{T}}) \, \bar{Y}_{nm}(\sigma),
\end{aligned}
\tag{9}
$$

Notconclusions (tempting but **false** conclusions)

- Since for any $P(r, \sigma)$ above S we have in $L_2(\omega)$ sense

$$
\begin{aligned}
V(P) &= \lim_{N_{\mathrm{T}} \to \infty} V_{N_{\mathrm{T}}}(P) \\
&= \lim_{N_{\mathrm{T}} \to \infty} \frac{GM}{\underline{R}} \sum_{n=0}^{N_{\mathrm{T}}} \left(\frac{R}{r} \right)^{n+1} \sum_{m=-n}^{n} \bar{V}_{nm}^{\mathrm{T}}(N_{\mathrm{T}}) \, \bar{Y}_{nm}(\sigma),
\end{aligned} \tag{9}
$$

so with your

$$
\lim_{N_{\mathrm{T}} \to \infty} \bar{V}_{nm}^{\mathrm{T}}(N_{\mathrm{T}}) = \left(\frac{\overline{R}}{\underline{R}} \right)^{n} \bar{V}_{nm}^{\mathrm{S}}, \tag{10}
$$

Notconclusions (tempting but **false** conclusions)

- Since for any $P(r, \sigma)$ above S we have in $L_2(\omega)$ sense

$$
\begin{aligned}
V(P) &= \lim_{N_{\mathrm{T}} \to \infty} V_{N_{\mathrm{T}}}(P) \\
&= \lim_{N_{\mathrm{T}} \to \infty} \frac{GM}{\underline{R}} \sum_{n=0}^{N_{\mathrm{T}}} \left(\frac{R}{r} \right)^{n+1} \sum_{m=-n}^{n} \bar{V}_{nm}^{\mathrm{T}}(N_{\mathrm{T}}) \, \bar{Y}_{nm}(\sigma),
\end{aligned}
\tag{9}
$$

so with your

$$
\lim_{N_{\mathrm{T}} \to \infty} \bar{V}_{nm}^{\mathrm{T}}(N_{\mathrm{T}}) = \left(\frac{\overline{R}}{\underline{R}} \right)^n \bar{V}_{nm}^{\mathrm{S}},
\tag{10}
$$

we get convergent satellite series for any $P(r, \sigma)$ above S

$$
\begin{aligned}
V(P) &= \frac{GM}{\underline{R}} \sum_{n=0}^{\infty} \left(\frac{R}{r} \right)^{n+1} \sum_{m=-n}^{n} \left(\lim_{N_{\mathrm{T}} \to \infty} \bar{V}_{nm}^{\mathrm{T}}(N_{\mathrm{T}}) \right) \bar{Y}_{nm}(\sigma) \\
&= \frac{GM}{\overline{R}} \sum_{n=0}^{\infty} \left(\frac{\overline{R}}{r} \right)^{n+1} \sum_{m=-n}^{n} \bar{V}_{nm}^{\mathrm{S}} \, \bar{Y}_{nm}(\sigma).
\end{aligned}
\tag{11}
$$

Notconclusions (tempting but **false** conclusions)

- Since for any $P(r, \sigma)$ above S we have in $L_2(\omega)$ sense

$$
\begin{aligned}
V(P) &= \lim_{N_{\mathrm{T}} \to \infty} V_{N_{\mathrm{T}}}(P) \\
&= \lim_{N_{\mathrm{T}} \to \infty} \frac{GM}{\underline{R}} \sum_{n=0}^{N_{\mathrm{T}}} \left(\frac{\underline{R}}{r} \right)^{n+1} \sum_{m=-n}^{n} \bar{V}_{nm}^{\mathrm{T}}(N_{\mathrm{T}}) \, \bar{Y}_{nm}(\sigma),
\end{aligned}
\tag{9}
$$

so with your

$$
\lim_{N_{\mathrm{T}} \to \infty} \bar{V}_{nm}^{\mathrm{T}}(N_{\mathrm{T}}) = \left(\frac{\overline{R}}{\underline{R}} \right)^{n} \bar{V}_{nm}^{\mathrm{S}},
\tag{10}
$$

we get convergent satellite series for any $P(r, \sigma)$ above S

$$
\begin{aligned}
V(P) &= \frac{GM}{\underline{R}} \sum_{n=0}^{\infty} \left(\frac{\underline{R}}{r} \right)^{n+1} \sum_{m=-n}^{n} \left(\lim_{N_{\mathrm{T}} \to \infty} \bar{V}_{nm}^{\mathrm{T}}(N_{\mathrm{T}}) \right) \bar{Y}_{nm}(\sigma) \\
&= \frac{GM}{\overline{R}} \sum_{n=0}^{\infty} \left(\frac{\overline{R}}{r} \right)^{n+1} \sum_{m=-n}^{n} \bar{V}_{nm}^{\mathrm{S}} \, \bar{Y}_{nm}(\sigma).
\end{aligned}
\tag{11}
$$

(False. Eqs. 9 and 10 hold but 11 does not, as $(\overline{R}/\underline{R})^n > 1$ for $n > 0$ in Eq. 10.)

- These effects can be seen with our current Earth gravity field models, so we are all doing it the wrong way.

- These effects can be seen with our current Earth gravity field models, so we are all doing it the wrong way.

  (False. The Earth seems to be too spherical and our data are too noisy to detect the differences between the satellite and terrestrial series reliably.)

- These effects can be seen with our current Earth gravity field models, so we are all doing it the wrong way.

  (False. The Earth seems to be too spherical and our data are too noisy to detect the differences between the satellite and terrestrial series reliably.)

- **Do not use spherical harmonics!**

- These effects can be seen with our current Earth gravity field models, so we are all doing it the wrong way.

  (False. The Earth seems to be too spherical and our data are too noisy to detect the differences between the satellite and terrestrial series reliably.)

- **Do not use spherical harmonics!**

  (False. Everybody should use spherical harmonics, because the fun is endless!)

Thank you for your attention!

References

Fukushima, T. (2017).
Precise and fast computation of the gravitational field of a general finite body and its application to the gravitational study of asteroid Eros.
The Astronomical Journal, 154(145):15pp.

Nolan, M. C., Magri, C., Howell, E. S., Benner, L. A. M., Giorgini, J. D., Hergenrother, C. W., Hudson, R. S., Lauretta, D. S., Margot, J. L., Ostro, S. J., and Scheeres, D. J. (2013).
Asteroid (101955) Bennu shape model V1.0. EAR-A-I0037-5-BENNUSHAPE-V1.0.
NASA Planetary Data System,
https://sbn.psi.edu/pds/resource/bennushape.html.

Backup slides

Solving Laplace's equation

$$\nabla^2 V(r, \sigma) = 0 \qquad (12)$$

in spherical coordinates r and $\sigma = (\varphi, \lambda)$ by separating variables leads to the external solid spherical harmonic expansion
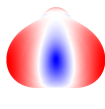
$$V(r, \sigma) = \frac{GM}{\overline{R}} \sum_{n=0}^{\infty} \left(\frac{\overline{R}}{r}\right)^{n+1} \sum_{m=-n}^{n} \bar{V}_{nm} \bar{Y}_{nm}(\sigma). \qquad (13)$$
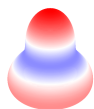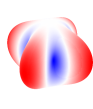

$\bar{Y}_{3,0}(\sigma)$ $\bar{Y}_{3,1}(\sigma)$ $\bar{Y}_{3,3}(\sigma)$ $\bar{Y}_{4,0}(\sigma)$ $\bar{Y}_{4,1}(\sigma)$ $\bar{Y}_{4,4}(\sigma)$

Motivation: Pitfall

Rescaling satellite coefficients in

$$V(r, \sigma) = \frac{GM}{\overline{R}} \sum_{n=0}^{N_{\mathrm{S}}} \left(\frac{\overline{R}}{r} \right)^{n+1} \sum_{m=-n}^{n} \bar{V}_{nm}^{\mathrm{S}} \, \bar{Y}_{nm}(\sigma) \tag{14}$$

from $\overline{R}$ to $\underline{R}$ by

$$\bar{V}_{nm}^{\mathrm{S}'} = \left(\frac{\overline{R}}{\underline{R}} \right)^{n} \bar{V}_{nm}^{\mathrm{S}}, \tag{15}$$

so that

$$V(r, \sigma) = \frac{GM}{\underline{R}} \sum_{n=0}^{N_{\mathrm{S}}} \left(\frac{\underline{R}}{r} \right)^{n+1} \sum_{m=-n}^{n} \bar{V}_{nm}^{\mathrm{S}'} \, \bar{Y}_{nm}(\sigma), \tag{16}$$

does not yield terrestrial coefficients, $\bar{V}_{nm}^{\mathrm{T}} \neq \bar{V}_{nm}^{\mathrm{S}'}$, nor does it change the behaviour of the series.

$\bar{V}_{nm}^{\mathrm{S}}$ and $\bar{V}_{nm}^{\mathrm{T}}$ are conceptually different and do not match.

Bennu: Characteristics of the model

Shape ratio $\overline{R}/\underline{R}$:
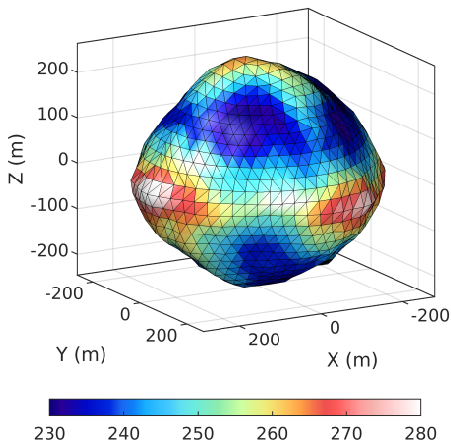- Bennu: 1.261
- Earth: 1.004
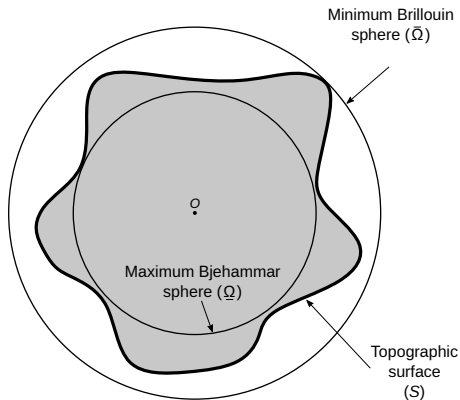
Shape ratio

Flat polygonal faces and sharp corners make polyhedral models
not suitable for our spherical harmonic study

Polyhedral shape model (m) due to [Nolan et al., 2013]

Parameters of the Bennu model and related constants

Density ρ (constant)	1260 kg m^{-3}
Shape S	$\bar{r}_{nm}^{\mathrm{S}}$ up to degree 15
Radius $\underline{R}$ of the Bjerhammar sphere $\underline{\Omega}$	224 m
Radius R of the mean sphere Ω	≈ 245.284 m
Radius R_{c} of the sphere of convergence Ω_{c}	≈ 282.5 m
Radius $\overline{R}$ of the Brillouin sphere $\overline{\Omega}$	283 m
Newton's gravitational constant G	6.67384×10^{-11} m^3 kg^{-1} s^{-2}

Satellite coefficients: Computation

Spectral gravity forward modelling ($\bar{r}^{\mathrm{S}}_{nm} \rightarrow \bar{V}^{\mathrm{S}}_{nm}$) evaluates Newton's integral

$$V(r, \sigma) = G \, \rho \iint\limits_{\sigma} \int\limits_{r'=0}^{r_{\mathrm{S}}} \frac{(r')^2}{\ell} \, \mathrm{d}r' \, \mathrm{d}\sigma \tag{17}$$

in the spectral domain, obtaining the satellite potential series

$$V(r, \sigma) = \frac{GM}{\overline{R}} \sum_{n=0}^{N_{\mathrm{S}}} \left(\frac{\overline{R}}{r} \right)^{n+1} \sum_{m=-n}^{n} \bar{V}^{\mathrm{S}}_{nm} \, \bar{Y}_{nm}(\sigma), \tag{18}$$

where

$$\bar{V}_{nm} = \bar{V}^{\mathrm{ball}}_{nm} + \bar{V}^{\mathrm{S,res}}_{nm}, \tag{19}$$

$$\bar{V}^{ball}_{nm} = \begin{cases} \frac{M_{\mathrm{ball}}}{M} & \text{for} \quad n = m = 0, \\ 0 & \text{otherwise}, \end{cases} \tag{20}$$

$$\bar{V}^{\mathrm{S,res}}_{nm} = \frac{4\pi \, \rho \, \underline{R}^3}{M} \frac{1}{2n+1} \left(\frac{R}{\overline{R}} \right)^n \sum_{p=1}^{p_{\max}} \frac{1}{p} \binom{n+2}{p-1} \bar{H}_{nmp}, \tag{21}$$

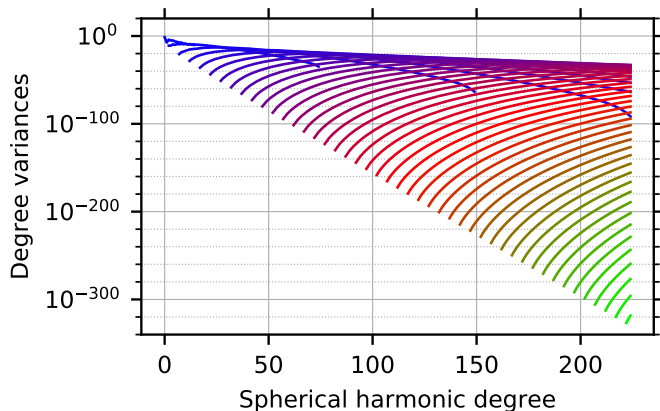$\bar{H}_{nmp}$ are spherical harmonic coefficients of the topography $H(\sigma) = (r^{\mathrm{S}}(\sigma) - \underline{R})/\underline{R}$ and M is the mass of Bennu. Despite r_{S} is limited to degree 15, the spherical harmonic expansion of the implied potential is infinite (in Eq. 18 truncated to N_{S}).
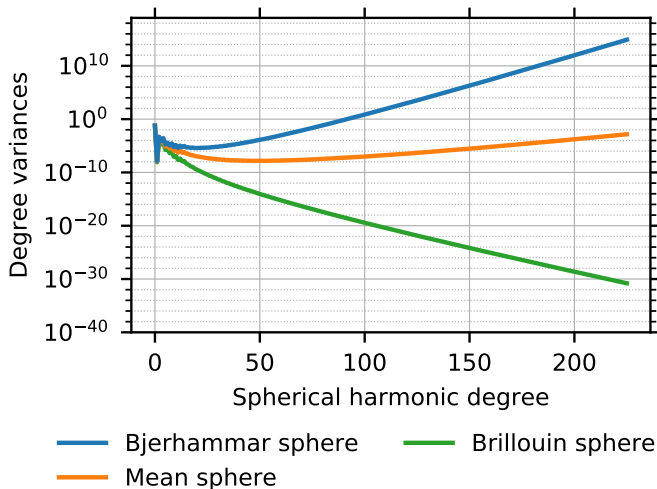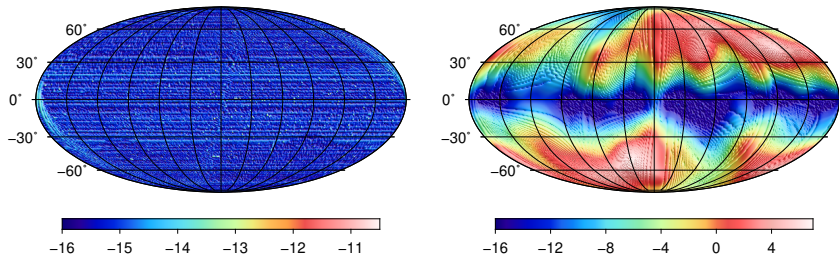
Spectrum obtained from the satellite spherical harmonic coefficients.
The spectra refer to three different spheres.

Spectra (dimensionless) of the gravitational contributions due to $H^p(\sigma)$ with $p = 1$ (light blue colour), 5, ..., 225 (light green colour). The spectra refer to the Brillouin sphere $\overline{\Omega}$.

Base-10 logarithm of relative errors between the potential from the satellite series and from spatial-domain gravity forward modelling after [Fukushima, 2017]. Left: Brillouin sphere, right: Bennu's surface.

- Surface gravitational data not available
- Given the closed-loop scenario, they can be computed with any accuracy
- Numerical integration technique after [Fukushima, 2017] applied
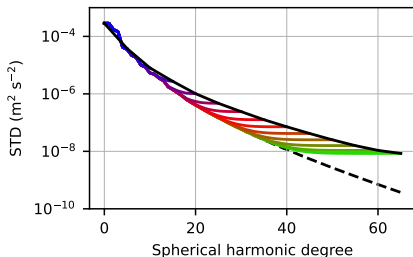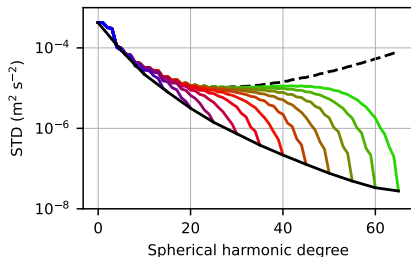- The computations took 90 CPU years while using 400 CPUs
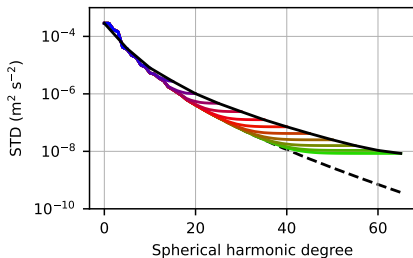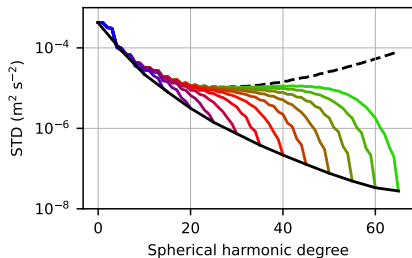
Spatial-domain errors of the terrestrial solutions (colour lines) and of the satellite solution (dashed black line) as a function of spherical harmonic degree.
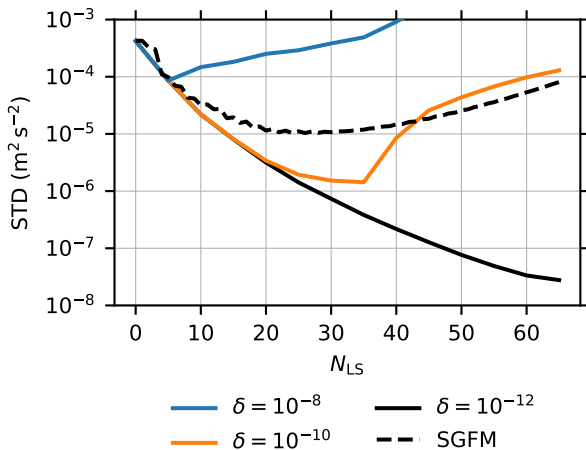*Left: Bennu's surface, right: Brillouin sphere.*

*Spatial-domain errors of the terrestrial solutions (colour lines) and of the satellite solution
(dashed black line) as a function of spherical harmonic degree.
Left: Bennu's surface, right: Brillouin sphere.*

Evaluating partial sums from terrestrial models
below the sphere of convergence can be dangerous.

Effect of the relative error tolerance δ on the right-hand side of Eq. (5). The terrestrial series were estimated for $N_{\mathrm{T}} = 0, 5, \ldots, 65$. For each model, the potential was synthesized using the full model, that is, with its maximum degree N_{T}. For a comparison, the dashed black line represents the satellite series. In all cases, the left-hand side of Eq. (5) is evaluated with $\delta = 10^{-16}$.
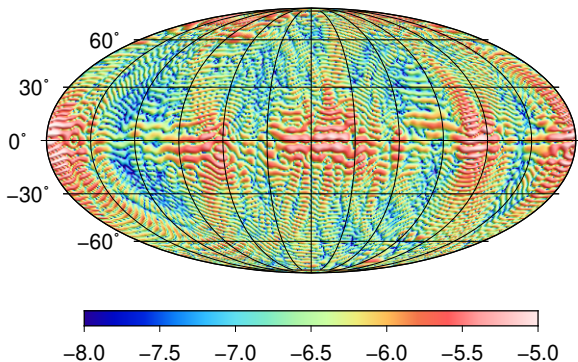
Validation of the terrestrial series with $N_{\mathrm{T}} = 65$ on the surface of Bennu in terms of the base-10 logarithm of relative errors. The synthesis was performed up to the maximum degree $N_{\mathrm{T}} = 65$ at the grid nodes of the Gauss–Legendre grid for degree 225.
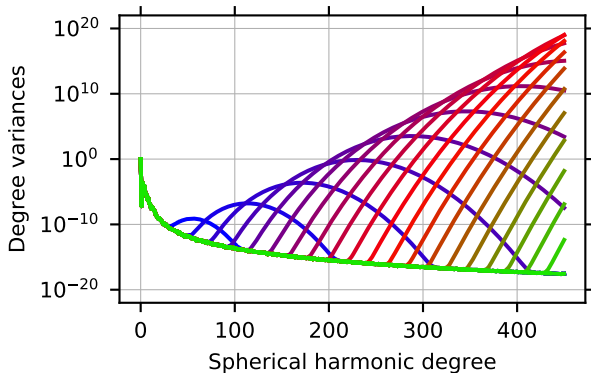
Degree variances (dimensionless) of $V_{\text{res}}^{\text{IE}} = V^{\text{Ext}} + V^{\text{Int}}$ plotted from the $\bar{V}_{nm}^{\text{Ext}}(R) + \bar{V}_{nm}^{\text{Int}}(R)$ coefficients up to degree 450. The curves show the spectrum at various levels of its completeness in terms of $p_{\max}^{\text{Ext}} = p_{\max}^{\text{Int}} = 10$ (blue curve), 20, 30, ..., 200, 1000 (green curve). Note that for the last curve with $p_{\max}^{\text{Ext}} = p_{\max}^{\text{Int}} = 1000$ (as well as for any $p_{\max}^{\text{Ext}} = p_{\max}^{\text{Int}} > 200$, not shown in the figure), no wave-like feature is visible within the studied bandwidth. The coefficients $\bar{V}_{nm}^{\text{Ext}}(R) + \bar{V}_{nm}^{\text{Int}}(R)$ were summed in quadruple precision to avoid underflow.
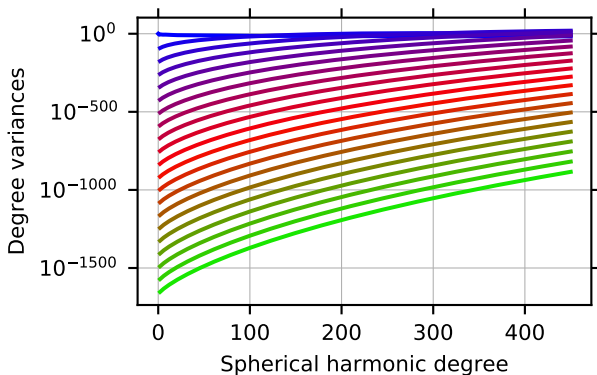
Spectra (dimensionless) of the gravitational contributions to V^{Int} made by the pth powers of $H^{(r_{\mathrm{S}} \geq R)}$ with $p = 1$ (blue colour), 50, 100, ..., 1000 (green colour). The spectra are shown up to degree 450 and refer to the mean sphere Ω. To avoid underflow, the quadruple version of the coefficients was used to prepare the figure.
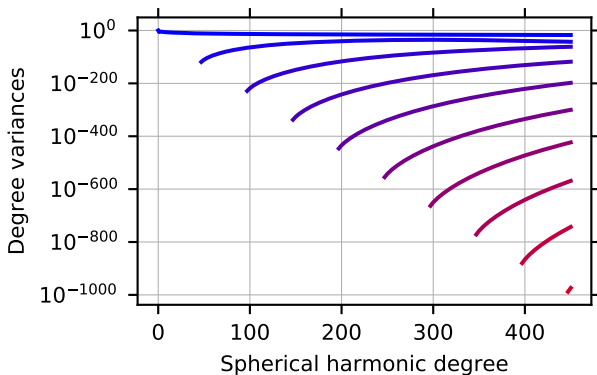
Spectra (dimensionless) of the gravitational contributions to V^{Ext} made by the pth powers of $H^{(r_{\mathrm{S}} \leq R)}$ with $p = 1$ (blue colour), 50, 100, ..., 450 (red colour). The same colour scheme is used as in the previous figure. Note that the powers $p > 453$ no longer contribute to the gravitational potential within the studied harmonic degrees. The spectra are shown up to degree 450 and refer to the mean sphere Ω. To avoid underflow, the quadruple version of the coefficients was used to prepare the figure.
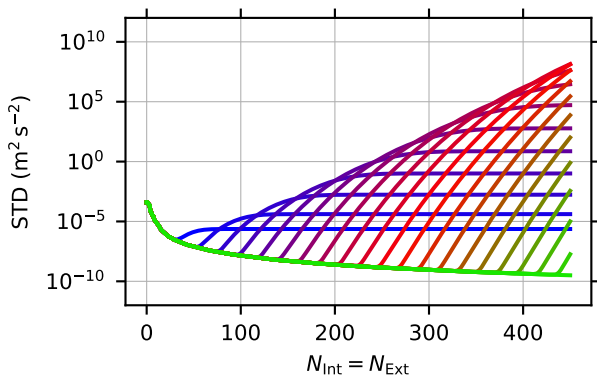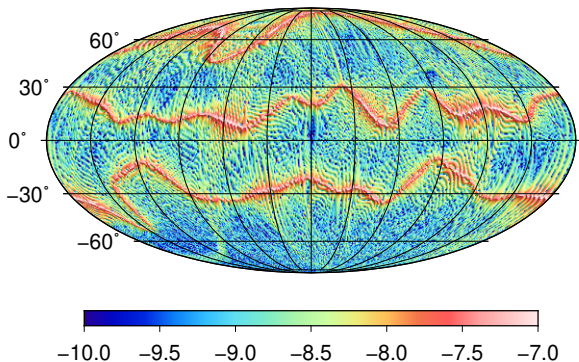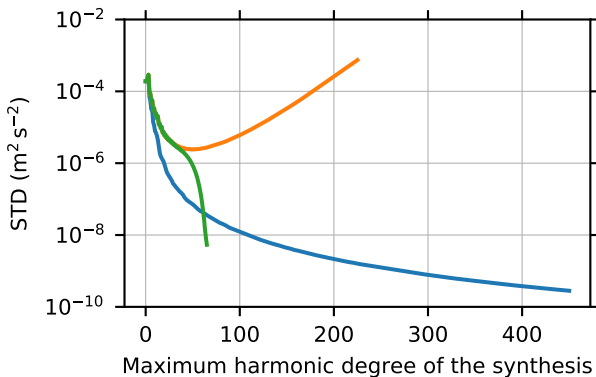
Validation of the internal and external series expansions against the reference gravitational potential on the mean sphere Ω. The standard deviations (STDs) of the discrepancies are shown for $p_{\max}^{\mathrm{Int}} = p_{\max}^{\mathrm{Ext}} = 10$ (blue colour), 20, 30, ..., 200, 1000 (green colour) as partial sums with increasing $N_{\mathrm{Ext}} = N_{\mathrm{Int}} = 0, 1, 2, \ldots, 450$.
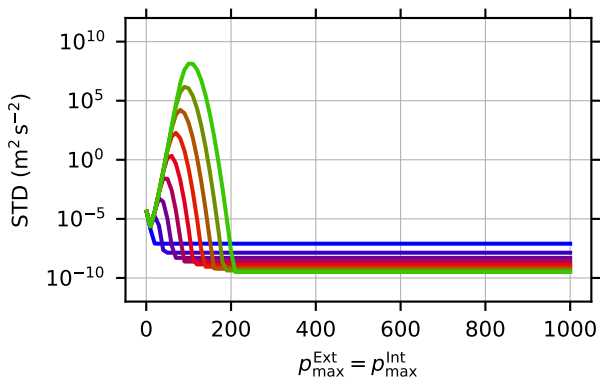
Validation of the internal and external series expansions on the mean sphere as a function of $p_{\max}^{\mathrm{Ext}} = p_{\max}^{\mathrm{Int}}$ with $N_{\mathrm{Ext}} = N_{\mathrm{Int}} = 50$ (the blue colour), 100, ..., 450 (the green colour). The following values of $p_{\max}^{\mathrm{Int}} = p_{\max}^{\mathrm{Ext}}$ were used: 1, 10, 20, ..., 250, 300, 400, 500, 750 and 1000.

Validation of the internal and external series expansions on the mean sphere using the base-10 logarithm of the relative errors. The synthesis was performed up to degree $N_{\mathrm{Ext}} = N_{\mathrm{Int}} = 450$ with $p_{\max}^{\mathrm{Int}} = p_{\max}^{\mathrm{Ext}} = 1000$. Note that some values exceed the scale of the colour bar. The true range is from about -13.6 to -6.5.

Validation of the studied techniques on the parts of the mean sphere that are external to the body: spectral gravity forward modelling (orange curve, N_S up to 225), least-squares estimation (green curve, N_T up to 65), and the combination of internal and external series expansions (blue curve, $N_{Ext} = N_{Int}$ up to 450, $p_{max}^{Int} = p_{max}^{Ext} = 1000$). The curves show the standard deviations of the differences between the three methods and the reference data from the spatial-domain Newtonian integration. Statistics of the reference gravitational potential at points on the mean sphere but outside the masses are (min, max, mean, STD, RMS): 2.064E−2, 2.161E−2, 1.907E−4 and 2.094E−2, respectively (all values in $\mathrm{m^2\,s^{-2}}$).